

ASSESSMENT OF HYPERSONIC MHD CONCEPTS

V. A. Bityurin and J. T. Lineberry
ERC Incorporated, Tullahoma, TN

V. G. Potebnia
Institute of High Temperatures of Russian Academy of Sciences (IVTAN)
Moscow, Russia

V. I. Alferov
Central AeroHydrodynamics Institute (TsAGI)
Moscow, Russia

A. L. Kuranov and E. G. Sheikin
Holding Company Leninetz, St. Petersburg, Russia

Abstract

MHD effects in air flow around a body moving with hypersonic velocity are considered. Simplified relationships for an on-board MHD flow control system are obtained and analyzed. A qualitative analysis of MHD systems for a scramjet optimization are presented. An experimental program to demonstrate MHD effects in hypersonic flow around a body is proposed. Such experimental studies can be performed in the MHD driven, hypersonic test facility of TsAGI. Estimations has shown that the significant MHD effects can be observed under the simulation condition of this facility. It is concluded that MHD flow control can be efficient in miscellaneous aerospace applications.

INTRODUCTION

A body moving through atmosphere with hypersonic velocity creates a system of strong shock waves. The shock waves formed are mainly responsible for a dramatic increasing in drag and huge heat flux into the body surface. These effects are significant technical problems that must be addressed for practical implementation of the hypersonic technologies [1,2].

However, intensive shock waves result in a significant ionization of the air flow in the viscous shock layer region. The latter effect allows in principle to use electrical and magnetic fields for control and optimization of the vehicle flowfield. The use of MHD control of the flow of weakly ionized plasmas created by strong shock waves was proposed and analyzed in 50s [3-4]. Recent interest in MHD aerospace application [5-10] has arisen. This interest has taken the form of emphasis on new approaches that were

developed in MHD electrical power generation as well as by the expectation/observations of the impact of weakly ionized plasma phenomena on supersonic/hypersonic aerodynamics [11].

During the last several decades similar technologies dealing with high speed flows of weakly ionized gases (equilibrium and non-equilibrium plasmas) in the presence of externally applied electrical and magnetic fields has been intensively developed (see, for example, 1st-34th Proceedings. of Symposium. on Engineering Aspects of Magnetohydrodynamics, Proceedings. of I-XII International Conferences on MHD Electrical Power Generation). This activity has mostly devoted to fundamental studies of magneto-gasdynamics flows as well as R&D on MHD energy conversion systems. The results of the MHD power R&D work over the past decades has resulted in well established knowledge base on the subject as well as a huge amount scientific and technical data. It can be contended therefore that the experience collected by the MHD power community (USA, Russia, Japan, etc.) on this subject should be extremely useful as a "jump start" for successful research in new MHD fields such as hypersonic aerospace technology.

The first requirement for the implementation of any on-board MHD technology is the choice of the magnetic system which is known to be a weight critical component. In this respect, the magnet size and weight must be gauged against the gain that can be obtained in terms of flow optimization. Some general relationships are obtained in this paper which should be useful for the development of a systematic approach to this problem.

concept. The results of estimation for this type of system, based on a simplified analysis, are discussed herein.

As a noted example of successful MHD application in hypersonic gasdynamics - the MHD driven wind tunnel, Hypersonic Test Facility at TsAGI (Moscow), is introduced and discussed. This facility is cited as one the long operating facilities in existence for MHD aerospace experimentation [12,13].

One of the most promising fields for MHD applications is MHD control of the bow shock characteristics. In particular, optimization of the drag to thrust ratio and/or a significant reduction in vehicle heat stress can be expected. Theoretical estimations and numerical simulation have shown that the bow shock configuration changes significantly when in the presence of an externally applied magnetic field. On the other hand, the reliable flow parameters prediction is still problematic due to a very complicated phenomena that occur in the vicinity of a hypersonic vehicle nose.

To demonstrate the qualitative/quantitative effects of a magnetic field applied in the bow shock region, a series of experimental studies is suggested. This experimental study can readily be performed in the experimental MHD facility of TsAGI (the Central AeroHydrodynamics Institute).

The principal features of the hypersonic flow and the diagnostic that are available at the TsAGI MHD facility are described in detail later and these can also be found in references 12 and 13. It is important note that realistic simulation of Mach number and static enthalpy behind the bow shocks can be demonstrated in this facility. Also, that external magnetic field strengths of a few to several Tesla can be created by pulse excitation using a simple coil located under the test model. This type of system has been successfully utilized in past experiments. The principal diagnostics needed to characterize the flow also exist including visualization of the flow structure, pressure, heat fluxes measurements.

ON-BOARD MHD FLOW CONTROL SYSTEM

Various aspects of the MHD flow control have been discussed in papers [1-10]. In our recent publications, the simplified concept of such a system is discussed [5-7,9-10]. The MHD flow control system (MHDFCS) under consideration consists of two main components: a magnet system that provides a desirable level of

magnetic induction in the interaction region; and, and MHD generator/accelerator represented by an electrode system installed on vehicle upstream surface. A proper load control subsystem is assumed to be available and its design and operation are outside of the scope of this paper but within current technology grasp.

An MHDFCS affects the flow in the hypersonic viscous shock layer by means of three field parameters defined by the three integral characteristics: integral electromagnetic body force \mathbf{F} acting in the flow and its corresponding reaction force $\mathbf{R}=-\mathbf{F}$

$$\mathbf{R} = -\mathbf{F} = \int_{\text{flow}} \mathbf{j} \times \mathbf{B} dV;$$

the integral moment,

$$\mathbf{K} = \int_{\text{vehicle}} \mathbf{r} \times \mathbf{f} dV;$$

and, the integral electrical power source/sink

$$Q = \int_{\text{flow}} \mathbf{j} \cdot \mathbf{E} dV.$$

Besides the aforementioned impacts MHD effects have on the flow, the MHDFCS influence is *implicit* through the flowfield modification caused by the local body force $\mathbf{f} = \mathbf{j} \times \mathbf{B}$ and local energy source/sink $q = \mathbf{j} \cdot \mathbf{E}$.

In the concept considered the magnetic system is assumed to be simulated by one- or two-wind coils zigzag shaped (see Fig.1 and Fig.2). This winding system provides a multipole magnetic induction distribution. The depth of the significant magnetic field penetration into the flow in normal-to-surface direction is defined by the period size of the winding in azimuthal direction.

Considering the hypersonic viscous shock layer as the most probable field for MHD influence, one can hypothesize that the most preferable winding configuration is that in which the characteristics thickness of the HVSL is used as the estimation for the half period size. It is assumed implicitly that the flow direction size of the winding considered is typically much greater than the azimuth period.

Two typical MHD interaction patterns might be considered. The first is when the interaction occurs in the vicinity of a flow directed portion of the winding (no even/odd difference). (Because of aforementioned remarks on size ratio this case is much more important.) The second pattern is when the flow in the vicinity of an azimuthal portion of the winding. Both are considered in analysis of following sections.

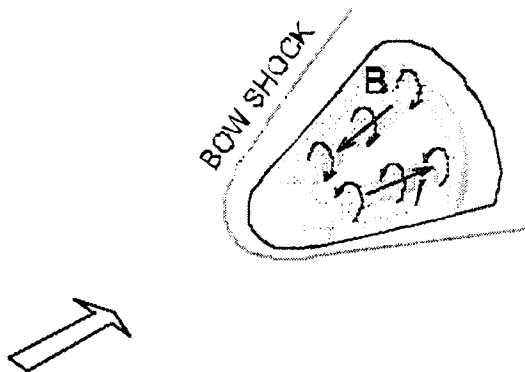


Fig.1 The schematic of the multiple magnetic system installed on a hypersonic spacecraft.

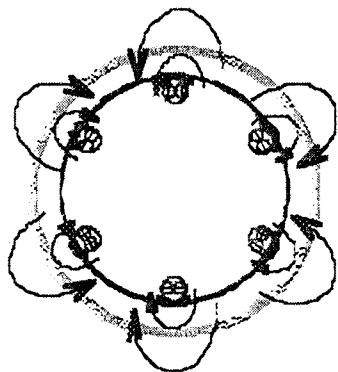


Fig.2. Cross-section view of the magnet system

Assuming for simplicity all flow parameters are constant and that the magnetic system is infinitely long in the flow direction, one can derive the following expressions for governing parameters

$$\begin{aligned} \mathbf{B} &= (0,0,B), \\ B &= B_0 \frac{r_0}{r}, \quad B_0 = \frac{\mu I_m}{2\pi r_0}, \\ \mathbf{j} &= (0,j,0), \quad \mathbf{E} = (0,E,0), \\ j &= \sigma(E - uB), \quad j = j^0 \frac{r_0}{r}, \\ i &= \int_0^{2\pi} j r d\theta = \text{const.} \end{aligned}$$

(A cylindrical reference frame is used with the x -axis in the flow and magnetic inductor current direction, r -axis in direction perpendicular to the magnetic inductor axis, and θ -axis as the azimuth direction.) In the above expressions, I_m is magnet current, r_0 is an apparent winding radius, u is x -component of the flow velocity, B is the θ -component of the magnetic induction, E is

the r -component of the electrical field strength, i is specific electrode current (per unit length).

For the short circuit case ($E=0$), the specific current is expressible as:

$$i \cdot 1m = R_m^{-1} I_m.$$

where R_m^{-1} is the magnetic Reynolds number for a 1.0 meter characteristics length.

The integral electromagnetic force integrated on the one meter domain can be estimated as

$$\begin{aligned} F_i &= R_m^{-1} \mu I_m^2 \zeta / G, \quad \zeta = \frac{1}{2\pi} \ln \frac{r^*}{r_0}, \\ P_{i,max} &= F_{i,max} u / 4. \end{aligned}$$

where r^* is the characteristics thickness of the interaction region and μ is the magnetic permeability. The condition required such that the MHD system is self sustained, e.g., the power consumed by the flight control systems is less than the power produced by MHD generator, is

$$\begin{aligned} \xi &= \frac{P_{MHD}}{P_{mag}} = \frac{\sigma_{mag}}{\sigma_{flow}} \text{Re}_m^2 \frac{\pi}{16G} \ln^2 \frac{r^*}{r_0} > 1, \\ \text{Re}_m &= \sigma \mu u r_0. \end{aligned}$$

where G is so called G-factor modified for the considered configuration. (Note, G-factor a measure of plasma non-uniformity used in MHD power technology.)

From the preceding expressions it is clear that interaction intensity is dependent on the magnetic system characteristics (total length of winding and inducing current I_m) and the flow parameters in the interaction region (typically- in the HVSL).

MPCE ENGINE FOR HYPERSONIC VEHICLE OF THE AJAX CONCEPT

A simplified schematic diagram of the AJAX MagnetoPlasmoChemical Engine (MPCE) is presented in Fig. 3. The MPCE is in fact a scramjet with MHD systems imbedded into the propulsion system.

The analysis of the scramjet performance characteristics conducted for the AJAX concept has shown that a considerable decrease of efficiency of a scramjet engine can be expected when the engine is operated at off-design conditions. This can be explained by the deterioration of

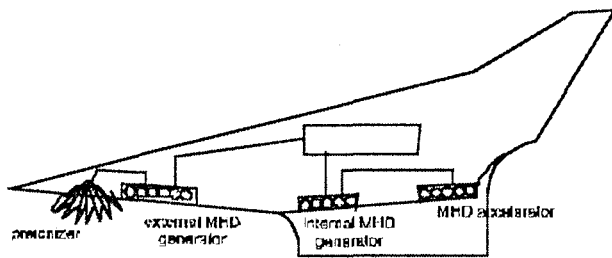


Fig.3. Schematic diagram of the AJAX concept vehicle with MHD system.

in-take mass flow rate and undesirable flow separation in combustor that occurs as well. Fitting the scramjet operating parameters to varying environment can be effectively provided using MHD flow control.

The conductivity of the oncoming flow behind the shock system is too low for significant MHD interaction when the flow Mach number is less than 10. For this reason, an artificial elevation of the electrical conductivity by use of preionization is needed. Preionization of intake air can be achieved by a variety of means including easily ionizing seed, microwave or corona discharge, e-beam and so on. In this study, an e-beam preionizing technique was assumed for the estimation of power consumption needed to provide the MHD interaction in the flow.

The analysis discussed below was conducted with the simplified quasi-one-dimensional model of the flow in the whole MPCE flow train (for details see [14,15]). The consequence of a pre-ionizer, an external MHD generator, a scramjet in-take, a combustor, an MHD accelerator and a nozzle was considered. For the case of preset electrical conductivity of the flow, it was found that a specific impulse in MHD application case can be increased by several percent. This is depicted in Figure 4.

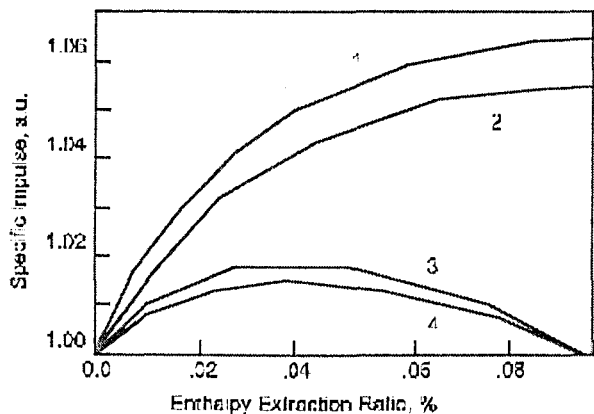


Fig.4. Specific impulse of MPCE vs. enthalpy extraction ratio. 1,2 - $M=6$; 3,4 - $M=8$; 1,3 - $\phi=0.95$; 2,4 - $\phi=1.0$.

For the self sustained system, wherein the conductivity pre-ionizer is driven by the power generated in the on-board MHD generator, third positive effect has been observed as well. In Figure 5, two cases are presented: curve 1 represents the operation mode when the net MHD generator power (above the pre-ionizer consumption) is put into the nozzle flow with MHD accelerator; and, curve 2 represents the case with the extra power utilization for other on-board needs.

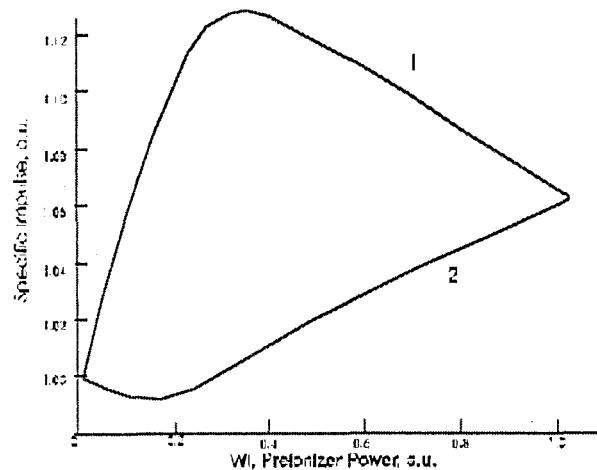


Fig. 5. Effects of MHD generator/accelerator on specific impulse of MPCE. 1- MHD generated electrical power consumed by the MHD accelerator; 2 - by on-board systems.

Only partial optimization procedure was used in this analysis and a much better result can be when the system is optimized in future planned studies.

EXPERIMENTAL STUDY OF HYPERSONIC FLOWS.

One of the main requirements for experimental study of hypersonic (hypervelocity) flows ($M \geq 12$) on ground test facilities is to provide the similarity of hypersonic velocity and density fields. Another important point in these laboratory studies for hypersonic flow is the real gas effects that become important in high Mach number regimes around complex aerodynamics objects [15].

In Fig. 6 the typical stagnation parameters P_{st} and T_{st} needed to reach desirable flow parameters (velocity and density) in the plenum chamber of a hypersonic wind tunnel are plotted.

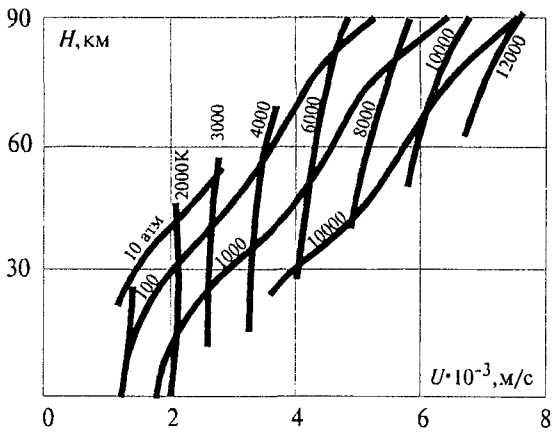


Fig.6. Inlet wind tunnel parameters needed for modeling flight conditions and calculated for adiabatic nozzle expansion.

For extreme test conditions, values of stagnation pressure greater than 1000 atm and stagnation temperature greater than 10,000K are necessary. This is a rather great technical problem for realization of a facility capable of simulation of hypersonic flows. Another problem raised in hypersonic experimental studies is the need to simulate the working gas composition in the test section. For these and other reasons, the utilization of an MHD gas accelerator for the experimental study of hypersonic (hypervelocity) flows was proposed many years ago [17,18].

One of the most successful operating MHD hypersonic facilities is located at TsAGI [19-22]. This facility is especially suitable for fundamental experiments to demonstrate MHD flow control. The working media (air) used in the TsAGI facility is seeded with alkali metal and provides elevated conductivity to the air plasma needed to effectively achieve an MHD interaction level over a rather wide range of operating parameters.

The TsAGI MHD test facility consists of following main elements:

- √ source of working (electrically conducting) gas with primary supersonic nozzle;
- √ MHD accelerator with magnetic system;
- √ secondary high Mach number nozzle;

- √ tests section with means for locating a tested model in the flow;
- √ diagnostics and control system.

A schematic of the TsAGI facility is presented in Fig. 7

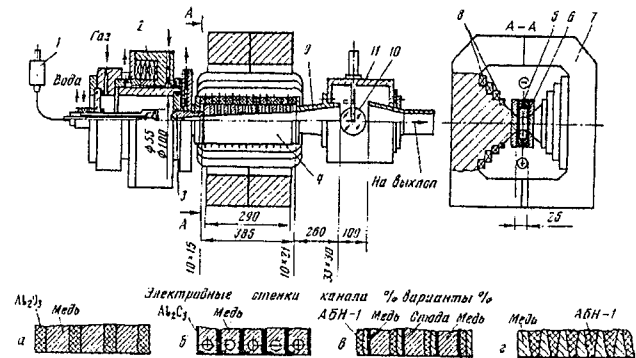


Fig. 7. Schematic diagram of the TsAGI MHD facility.

The electrical power of the facility in the range of operating parameters is $p=0.1-2\text{MPa}$, $T=3000\text{K}-6000\text{K}$, with mass flow rate $0.02-0.25\text{kg/s}$ is correspondingly $0.2-2\text{MW}$. There is capability to provide values of $T=5000\text{K}$ and $p=20\text{MPa}$ in the source of the hot plasma flow.

The detailed technical and operating characteristics of this facility are discussed in papers [12,13,19-22]. As a rule, experimental runs are carried out with flow of air that is seeded with 1% of $K-Na$ eutectic. The state at the accelerator inlet is $T=2700\text{K}$, $u=1900\text{m/s}$, $M=2$, static pressure $p=0.2-0.5\text{atm}$ depending on air mass flow rate.

Aerodynamic measurements include static pressure distribution in the test section, static pressure at the secondary nozzle exit cross-section, and, the pressure distribution on the model surface in the test section.

Visualization of the hypersonic flow field, shock waves structure and its evolution in time, are also available at MHD facility. One example of the visualization of the flow around a TAV Bor-4 model is presented in Fig. 8.

MHD DEMONSTRATION EXPERIMENT

Basing on the existing capabilities of the TsAGI MHD hypersonic facility (MHD HTF) a near term program for experimental study of aerospace MHD effects can be formulated. This can encompass laboratory flow visualization and measurements for high supersonic or hypersonic flow around aerodynamic shapes or aerospace



Fig. 8 An example of visualization of the hypersonic viscous shock layer on a TAV model.

models in hypersonic viscous shock layer as well as in the near wake and behind an obstacle.

GENERAL DEMANDS

In order to demonstrate successfully expected MHD effects one can provide the experimental conditions under which so-called MHD interaction parameter

$$S = \frac{\sigma B^2 l}{\rho u}$$

should be high ($S > 1$). In the preceding expression, l stands for a characteristics length, B is magnetic induction, and σ , ρ , u are the flow parameters: conductivity, density and velocity, respectively.

The characteristics length l is limited in the case under consideration by the size of the test section of the experimental facility and can be estimated as high as 0.2 m. The magnetic induction is represented by the value averaged over the interaction region. It was found that B-field levels of 1T - 2T can be available with a simple pulsed type magnetic system.

The electrical conductivity σ is considered as the thermal equilibrium conductivity of the air seeded with an alkali metal. For the conditions typical of the experimental test facility operation mode the conductivity in the interaction region are in the range of 100 mho/m - 1000 mho/m.

The mass flow flux density ρu is defined mainly by the stagnation parameters : pressure $p_{st} \cong 10^7$ - 10^8 Pa, $T_{st} \cong 1000$ K. and by Mach number. In the interaction region (behind the bow shock) is it computed to be as high as $10 \text{ kg/m}^2 \text{ s}$ - $100 \text{ kg/m}^2 \text{ s}$.

Therefore, the MHD interaction parameter is around one which is high enough for significant demonstration experiment. The representative series of experiments can be organized in a fashion to discretely study MHD influence on the flow, i.e., the stagnation parameters are fixed and the MHD interaction effects are perturbed to study variation of the controlling parameters and the model geometry.

MODEL GEOMETRY

One of the simplest aerodynamics body - a wedge with varying angle has been chosen for this experimental series. The rather high value of the angle (30° , 45° , 60° and 90°) can provide a significant variation of the static parameters behind the shock and consequently the significant variation of the interaction.

The schematic diagram of the model equipped with a single wind pulsed type magnetic system is presented in Fig. 9. The effective cross-section diameter of the winding is chosen as high as 0.01m. The two opposite directed turns of the winding are placed just under the model upstream surface at the distances from the wedge axis of 0.05m and 0.15m consequently. The peak electrical current of 100 kA provides an average magnetic induction in the interaction region at a level of 1 Tesla.

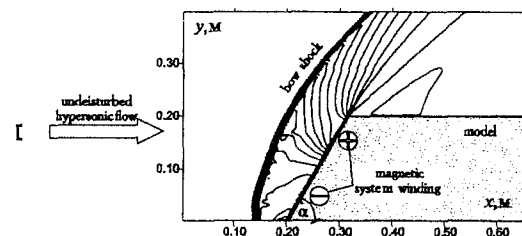


Fig. 9. Schematic diagram of calculation domain of the MHD test section.

MODEL MAGNETIC SYSTEM

The schematic diagram of the model equipped with a single wind pulsed type magnetic system is presented in Fig. 9. The effective cross-section diameter of the wind is chosen as high as 0.01m. The two opposite

directed turns of the wind are placed just under the model upstream surface at the distances from the wedge axis of 0.05m and 0.15m consequently. The peak electrical current of 100 Kay provides the average magnetic induction in the interaction region at the level of 1T.

MOMENTUM AND ENERGY CONVERSION CONTROL IN HVSL

The momentum and energy conversion control in hypersonic viscous shock layer (HVSL) can be provided with an externally applied electric field by controlling the electrical current distribution in the interaction region. For this purpose, additional electrodes should be installed on the model surface. In the geometry presented in Fig. 9 electrodes are placed in front of and behind the schematic plane (invisible in the sketch). These electrodes provide a net current, I , and an external voltage, V . Together, these two parameters define the net power $P = IV$. The value of the net current is defined as the integral of the current density vector component normal to the plane of the sketch.

$$I = \iint j_z dx dy.$$

Experimental evidence of the MHD flow control efficiency can be obtained with Voltage-Current Characteristic (VCC) as the dependency of the net current I upon the net voltage V . At the same time, the electrical power extractable from the oncoming flow with an MHD on-board generator system can be estimated as well.

PREDICTION

In the previous sections it was elucidated that the governing parameters of the TsAGI MHD hypersonic test facility allow the capability to conduct representative and informative experimental series to demonstrate MHD effects in the hypersonic flows around aerodynamics models/shapes. Using simple model geometry and easy-to-analyze magnetic field distributions present desirable conditions for applications of the well developed numerical methods to qualitative and quantitative analysis of the MHD interaction processes in the test section.

This type of analysis was performed in preparation of this paper and the numerical model exercised to provide the preliminary analysis given herein. The analysis technique used can provide experimental prediction and it has been validated against analytical studies of gas-

plasma interacting flows [23-27]. For this reason the results discussed in the following section are considered at least to be qualitatively reliable. Moreover, the authors' note that quantitative characteristics of the modeling flow can differ significantly from those of the full scale processes on a real aerospace vehicle moving through the atmosphere with hypersonic velocities. The main reasons of this are surface and real gas phenomena.

NUMERICAL MODELING

In the numerical study of the experimental result prediction a zero angle-of-attack wedge with the various of the divergence angle is considered. It is assumed that the magnetic system is placed as previously described. The magnetic induction is a two component vector

$$\mathbf{B} = \{B_x, B_y, 0\}$$

with

$$B = B_0 r_0 / r,$$

where B_0 is the absolute value of magnetic induction on the effective radius of the wind r_0 .

The induced electrical current is perpendicular to the consideration plan

$$\mathbf{j} = \{0, 0, j_z\}.$$

It is assumed that the problem is two dimensional.

The governing equation are:

Euler's equations

$$\begin{aligned} \frac{\partial \rho}{\partial t} + u_x \frac{\partial \rho u_x}{\partial x} + u_y \frac{\partial \rho u_y}{\partial y} &= 0, \\ \frac{\partial \rho u_x}{\partial t} + u_x \frac{\partial (\rho u_x^2 + p)}{\partial x} + \frac{\partial \rho u_x u_y}{\partial y} &= f_x, \\ \frac{\partial \rho u_y}{\partial t} + u_y \frac{\partial (\rho u_y^2 + p)}{\partial y} + \frac{\partial \rho u_x u_y}{\partial x} &= f_y, \\ \frac{\partial e}{\partial t} + \frac{\partial (e+p)u_x}{\partial x} + \frac{\partial (e+p)u_y}{\partial y} &= q, \end{aligned}$$

where

$$e = \rho (c_v T + (u_x^2 + u_y^2) / 2),$$

$$T = p / R\rho.$$

Generalized Ohm's law in the simplest form

$$\mathbf{j} = \sigma (\mathbf{E} + \mathbf{u} \times \mathbf{B})$$

and the right hand side of Euler's equations are

$$\begin{aligned} \mathbf{f} &= \{f_x, f_y, 0\}, \\ \mathbf{f} &= \mathbf{j} \times \mathbf{B}, \\ q &= \mathbf{j} \cdot \mathbf{E} \end{aligned}$$

The electrical conductivity is calculated as follows:

$$\sigma = \sigma_1 \sigma_2 / (\sigma_1 + \sigma_2),$$

where

$$\begin{aligned} \sigma_1 &= 1.83 \times 10^5 (T)^{3/4} \exp(-2.6 \times 10^4 / T), \\ \sigma_2 &= 15085 \times 10^{-2} T^{3/2} / \ln \Lambda \\ \Lambda &= 1.2989 \times 10^7 T^{3/2} n_e^{-1/2}. \end{aligned}$$

The electron density n_e is calculated on Saha' equation. The boundary conditions are non-disturbed transparency conditions on all upstream borders and the reflective conditions on the wedge surface as well as on the symmetry line.

DISCUSSION

Typical results of numerical modeling are presented in Fig. 10 - Fig. 18.

The reference flow case without magnetic field is illustrated by the static pressure and x-component velocity distributions presented in Fig. 10 and Fig. 11 respectively. It is clearly seen that the flowfield calculated in this study corresponds to very well known in the literature. Under considered conditions ($M_\infty \approx 15$ and $\alpha = 60^\circ$) the bow shock is stand-off the wedge surface. The temperature in the shock layer is about 7000K and the static pressure is about 2.0 kPa. For this condition, the electrical conductivity is calculated to be in the range of 100 mho/m - 1000 mho/m.

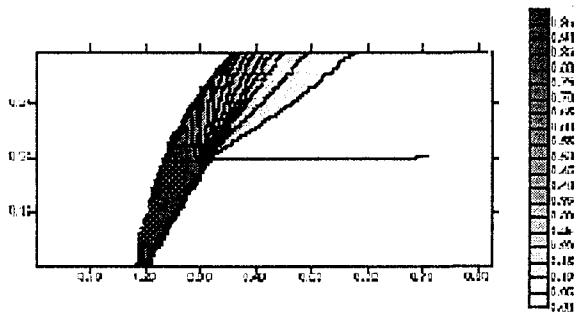


Fig 10. Normalized static pressure p/p_{max} distribution in state flow around a wedge ($\alpha=60^\circ$). $B=0, E_z=0, u_\infty=5000m/s, p_{max}=208KPa$.

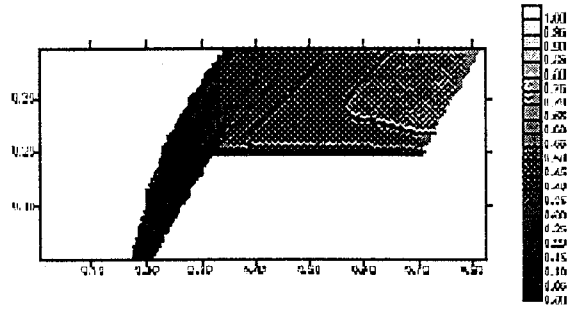


Fig. 11. Normalized x-component velocity distribution u/u_∞ under conditions of Fig. 10

The first MHD interaction case is the “short circuit” operation mode when the external applied voltage is equal to zero ($E_z=0$) and nominal magnetic field has been applied. The static pressure and x-component flow velocity are presented in Fig. 12. and Fig. 13.

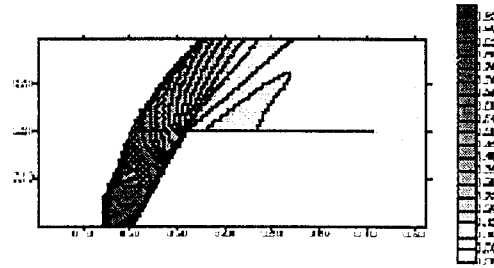


Fig. 12. Normalized static pressure p/p_{max} distribution in state flow around a wedge ($\alpha=60^\circ$). $B=B_{nom}(x,y), E_z=0, u_\infty=5000m/s, p_{max}=208KPa$.

Due to the MHD interaction that is represented by electromagnetic body force $\mathbf{j} \times \mathbf{B}$ while the energy

source is equal to zero the flowfield has disturbed significantly. The bow shock location is changed and stand-off parameter is increased several times. The static pressure distribution has been significantly changed and the pressure gradient drop has appeared in upstream region. It is interesting to note that because of the very conservative behavior of the maximal pressure (it is approximately equal to the pressure in the critical point behind the bow shock) the appears of the pressure gradient results in decreasing of the average static pressure in the shock layer. Thus the “pressure” component of the drag is decreased. At the same time the electromagnetic interaction between the flow and the magnetic system has appeared [8]. This interaction can be defined by the formula

$$\mathbf{R} = -\mathbf{F} = \iint_{\text{flow}} \mathbf{j} \times \mathbf{B} ds$$

It was found that in the case under consideration the decreasing of the “pressure” drag calculated as

$$F_p = - \int_{\text{wedge surface}} p \mathbf{n} dl$$

is approximately “compensated” by increasing of the electromagnetic drag force \mathbf{R} .

The distribution of the current density is defined in this case only by the local values of conductivity and electromotive force. The current density distribution is presented in Fig. 14.

The maximal value of the current density is as high as 125A/cm² occurred near the wedge critical point with the maximal temperature and in the vicinity the turn-off location where the velocity becomes high while the temperature and magnetic field are still high as well. It is important to note that the sign of the current density alters at these locations that corresponds to the magnetic induction direction.

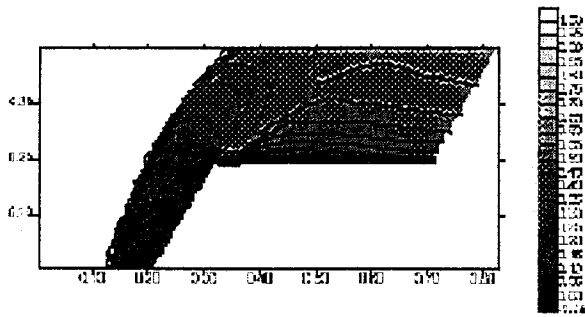


Fig. 13. Normalized x-component velocity distribution u/u_∞ under conditions of Fig.12

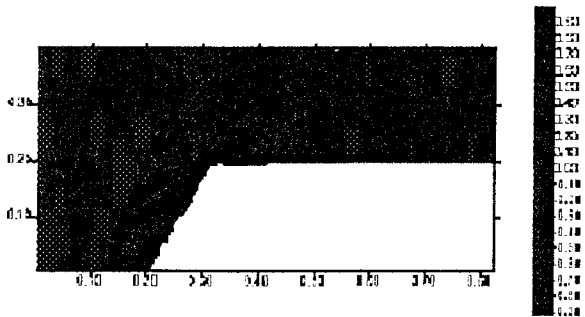


Fig. 14. Normalized z-component current density distribution j_z/j_{max} under condition of Fig.12. $j_{max}=125A/cm^2$.

The total short circuit current which is calculated as integral of the current density j_z over whole domain is found as high as 10 kA.

It is found that under considered in this study conditions the voltage current characteristics are practically linear. The apparent linearity of MHD processes even in strong interacting flow is very well known fact in the MHD generator analysis.

In this case it help us to define the maximal power output conditions with $I=I_{sc}/2$ and, consequently, $V=V_{os}/2$. The optimal electric field strength is found as high as $E_z = -40$ V/m.

The corresponding numerical results are presented in Fig. 15-Fig. 17. It is seen that the flowfield seems to be rather similar to the previous MHD interacting flow. The effect of energy extraction from the flow is small. The power output can be estimated as

$$Q = 5000 \times 40 \times 0.2 = 40 \text{ kW}$$

that is less than 1% of the total enthalpy flux.

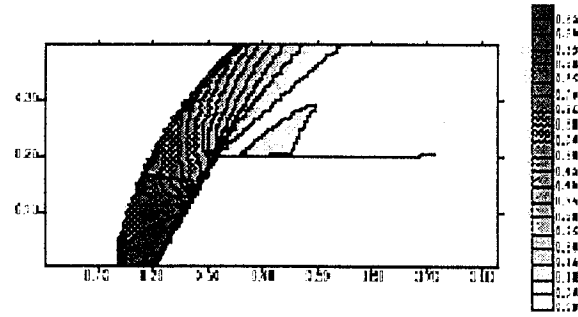


Fig. 15. Normalized static pressure p/p_{max} distribution in state flow around a wedge ($\alpha=60^\circ$). $B=B_{nom}(x,y)$, $E_z=-40V/m$, $u_\infty=5000m/s$, $p_{max}=208KPa$.

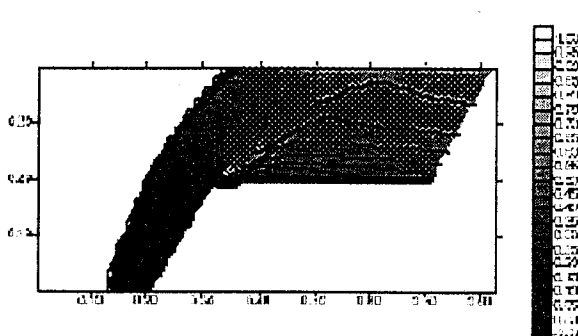


Fig. 16. Normalized x-component velocity distribution u/u_∞ under conditions of Fig.15

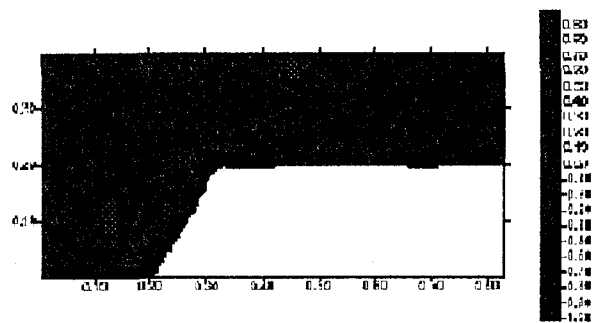


Fig. 17. Normalized z -component current density distribution j_z/j_{max} under condition of Fig. 15. $j_{max}=105A/cm^2$.

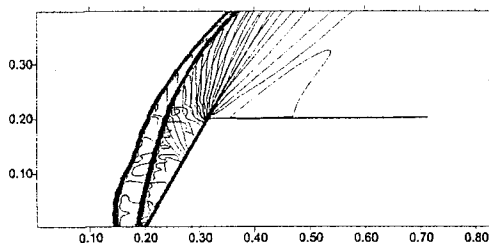


Fig. 18. Comparison of static pressure distributions under conditions of Fig. 10 ($B=0$) and Fig.12 ($B=B_{nom}$).

In Fig. 18 the static pressure distributions of non-MHD and short circuit cases are compared. The main effect of the MHD interaction is clearly seen: the bow shock stand-off has increased in several time. The MHD interaction on heat transfer will be studied later.

CONCLUDING REMARKS

Preliminary assessments, such as that herein and others, of various magnetohydrodynamics processes for application to aerospace systems have shown that the existing technology is quite promising. In this context, we emphasize that extended theoretical, experimental and conception studies are needed to provide more details on the exact prospectus of MHD for advanced aerospace applications.

With the renewed interest in the aerospace community on possible plasma effects and MHD flow control, the authors' stress to the community that there is a wealth of knowledge on these subjects available through the MHD power community. Large scale, worldwide MHD power research had been on-going for over thirty years

and this knowledge base and experience should be taped as a resource for developing aerospace applications.

The analysis of MHD effects in hypersonic flow behind bow shock has shown that the operation conditions of the TsAGI MHD Hypersonic Test Facility (or any similar on scale and operating conditions) are rather suitable to provide significant MHD interaction in such a flow. This facility is operational and simple experiments such as the type posed herein could be readily and quickly accomplished to provide near term evidence of plasma and MHD effects; such as, shock dissipation and drag reduction. These effects can be detected with available diagnostics at TsAGI and treated/studied with state-of-the-art numerical methods.

MHD flow control seems to be rather promising for miscellaneous aerospace applications.

The reliable models of surface and gas phenomena are to be very important for detailed quantitative description of the flow characteristics.

REFERENCES

1. Dertin, John J., "Hypersonic Aerothermodynamics", AIAA Educational series, 1994
2. G.G.Tcherny, Gasdynamics, 1987, Moscow, (Russian)
3. A. R. Kantrowitz, *A Survey of Physical Phenomena Occurring in Flight at Extreme Speeds*. Proc. Conf. on High Speed Aeronaut., N.Y., 1955, p.335.
4. W.Bush, J.Aero/Space Sci., Vol.25,685-690 (1958)
5. A. Kh. Mnatsakanian, G. V. Naidis, *On MHD Effects on Spacecraft Motion in the Earth Atmosphere*, Research Report 92/11, IVTAN, 26p, 1991 (in Russian).
6. V. A. Biturin, V. A. Ivanov, A. N. Botcharov, N. N. Klutchnikov, *Magnetogasdynamics Control of Spacecraft Motion in the Upper Atmosphere*, Research Report IVTAN-ANRA 94/3, 1994, Moscow, p. 37 (in Russian).
7. V. A. Biturin and V. A. Ivanov, *An Alternative Energy Source Utilization with an MHD Generator*, In: 33rd Symp.on Eng. Aspects of MHD, June 13-15 1995, UTSI, Tullahoma, TN, p.X-2.1.
8. J. Cole, J.Campbell, and A.Robertson, *Rocket-Induced Magnetohydrodynamic Advanced Propulsion Concept*, AIAA Paper 95-4079.

10. E. P. Gurjanov and P. T. Harsha, *AJAX: New Directions in Hypersonic Technology*, AIAA Paper 96-4609.
11. Weakly Ionized Gases Workchop, 9-13 June 1997, USAF Academy, Colorado.
12. V. I. Alferov. *MHD-Gas Accelerators for Hypersonic Wind Tunnels. History of Development, Current Status and Prospects.* // Twelfth International Conference on Magnetohydrodynamic Electrical Power Generation, v1, pp.423-434.
13. V. I. Alferov, L. M. Dmitriev, B. V. Yegorov, Yu. Ye. Markachev, and A. P. Rudakova. *On the Possibility of Reproducing Flight Conditions for Transatmospheric Vehicles in Hypersonic MHD-Gas Acceleration.* // Twelfth International Conference on Magnetohydrodynamic Electrical Power Generation, v1, pp.435-444.
14. E. G. Sheikin, *An Analytical Solution of the MHD equation set in quasi-one-dimensional approximation with monatomic parameters variation along the channel. I.* Technical Physics, Vol.62, No 12, 1992.
15. E. G. Sheikin, *An Analytical Solution of the MHD equation set in quasi-one-dimensional approximation with monotonic parameters variation along the channel. II.* Technical Physics, Vol.63, No 9, 1993.
16. F. Jaarsma, W. B. de Wolf. AGARD - R-600.
17. G. Wood, A. Carter. ARS-Paper No. 903-59, 1959.
18. G. Wood, A. Carter, In: *Ionic, Plasma and Arcjet Rocket Engines*, GosAtomIsdat, 1961(in Russian).
19. V. I. Alferov., O. N. Vitkovskaya., V. P. Rukabetz., G. I. Scherbakov, In: *Electroarc Gas Heaters*, TsAGI Proc, 1978 (Russian).
20. Alferov, O. N. Vitkovskaya, Yu. S. Ustinov, G. I. Scherbakov , *Teplofizika Vysokikh Temperatur*, Vol.9, No 2, 1971 (see also High Temperatures, 1971).
21. V. I. Alferov, O. N. Vitkovskaya, Rukavetz V. P., G. I. Scherbakov , *Teplofizika Vysokikh Temperature*, Vol 7, No 1, 1979 (see also High Temperatures, 1979).
22. V. I. Alferov, O. N. Vitkovskaya, A. P. Rudakova., G. I. Scherbakov , *Teplofizika Vysokikh Temperatur*, Vol 17, No 2, 1979 (see also High Temperatures, 1979).
23. V. I. Alferov, A. P. Labazkin, A. P. Rudakova, G. I. Scherbakov. *Applications of MHD Accelerators in Hyper-Velocity Experimental Aerodynamics.* // Eleventh Intern. Conf. on Magnetohydrodynamic Electrical Power Generation, 1992, Beijing, China, October 12-16, vol.4, p.1308.
24. V. A. Bityurin, A. P. Likhachev, G. A. Lyubimov, S. A. Medin, *Izvestiya AN SSSR. Mekhanika gidkosty i gasa*, 1989, No 5, pp 135-145 (see also Fluid Dynamics, 1989).
25. V. A. Bityurin, A. P. Likhachev, *Numerical Study of the Processes in the MHD Generator with STCC Non-Uniformities. Quasi-Two-Dimensional Approximation.* // In: Eleventh International Conference on Magnetohydrodynamic Electrical Power Generation, 1992, Beijing, China, October 12-16, vol.III, p.785.
26. V. A. Bityurin, V. A. Ivanov, A. Veefkind, *Teplofizika Vysokikh Temperatur*, Vol.33, No 5, 1995 (see also High Temperatures, 1995).
27. A. P. Likhachev, *Numerical modeling nonuniform and non-steady state flows in a supersonic MHD channel*, Thesis, IVTAN, Moscow, 1989 (Russian).